Optimized Precoders for Vehicular Massive MIMO RadCom Systems

Murat Temiz[1], Emad Alsusa[1], and Mohammed W. Baidas[2]
[1]School of Electrical and Electronic Engineering, University of Manchester, Manchester, UK
[2]Department of Electrical Engineering, Kuwait University, Kuwait
(e-mail: {murat.temiz, e.alsusa}@manchester.ac.uk, m.baidas@ku.edu.kw)

***Abstract*—This paper proposes optimized precoders for dual-functional radar and communication (RadCom) systems to maximize the sum-rate (SR) while satisfying radar target detection and user data rate constraints towards 6G networks. For this purpose, a RadCom precoder scheme that exploits radar interference is utilized with massive multiple-input-multiple-output (MIMO) orthogonal frequency-division multiplexing (OFDM) systems. Firstly, the communication capacity and radar detection performance metrics are analytically derived. Then, optimum precoders that utilize these analytical expressions are designed via convex optimization to maximize the SR with modest computational complexity. The analytical results are also verified by simulations. The results show that the optimized precoder can substantially enhance the SR compared to the benchmark methods.**

***Index Terms*—Massive MIMO, radar and communication, OFDM radar, 6G networks, spectrum sharing, power allocation**

I. Introduction

Automotive radars and communication systems are expected to be essential parts of intelligent transportation systems and supported by 6G networks. Specifically, an autonomous driving vehicle has to communicate with its surrounding (e.g. other vehicles, road side units (RSU) or pedestrians), and sense the road conditions in order to safely and effectively operate. However, both high-data rate communications and precise radar sensing require large bandwidth, and hence, may cause congestion in the frequency spectrum and interference between the two systems. Thus, various methods have recently been proposed to enable joint radar sensing and communication [1]. Particularly considering vehicular systems, a short-range radar and robust communications supporting vehicle-to-vehicle (V2V), vehicle-to-network (V2N) or vehicle-to-everything (V2X) transmissions are necessary [2]. To facilitate joint radar and communication functions on the same platform, coordinated signaling or dual-functional waveforms can be employed. Coordinating signaling may be achieved by time or frequency division allocation between radar and communication signals, or beamforming towards the user equipments (UEs) and targets. Alternatively, the communication signals may be utilized for sensing, or radar waveforms can convey information to the UEs. For instance, radar waveforms utilizing linear frequency modulation (LFM), continuous phase modulation (CPM), and quadrature amplitude modulation (QAM) were considered for data transmission [3]. The spatial diversity offered by large-scale antenna arrays was also exploited for dual-functional radar and communication systems [4]. OFDM waveforms have also been considered for vehicular system RadComs due to their flexibility in signal processing [5]. For example, OFDM waveforms for vehicular radar and communications were studied in [5] and [6]. Moreover, an interference mitigation algorithm was proposed to alleviate the interference caused by the Doppler shift and/or non-ideal hardware components [7]. In [8], a continuous-wave massive MIMO OFDM RadCom architecture with a novel precoder was proposed by utilizing all the subcarriers for communications and radar simultaneously, and exploiting interference. Specifically, an omnidirectional radar sensing is used for sensing, while the communication data is beamformed onto UEs.

In this study, a new precoder scheme is proposed to maximize the sum-rate (SR) by selecting the optimum radar and communication power outputs, as well as, optimizing the beam power allocation to the UEs based on our proposed RadCom architecture in [8]. Furthermore, analytical expressions for the communication capacity and radar SINR of our proposed RadCom architecture are derived under practical network conditions, where the UEs and targets may have significantly different channel gains. Simulation results are presented to illustrate the superior performance of the proposed scheme in comparison to benchmark techniques.

Notation: Throughout the paper, the following notation is used. Bold uppercase letters (e.g. $\mathbf{H}$) indicate matrices while bold lowercase letters (e.g. $\mathbf{h}$) indicate vectors. Superscripts *,^{T}, ^{H} indicate the conjugate, transpose and Hermitian transpose, respectively. Subscripts $_{com}$ and $_{rad}$ relate the corresponding parameter to communication or radar (e.g. $\mathbf{H}_{com}$ and $\mathbf{H}_{rad}$), respectively. The absolute value, Euclidean norm, Frobenius norm and expectation operators are denoted by $|.|$, $\|.\|$ and $\|.\|_F$, $\mathbb{E}[.]$, respectively.

II. System Model

Fig. 1 depicts the considered RadCom system, where a single BS with M antennas communicates with K downlink UEs, while the single radar transmit antenna omnidirectionally transmits an OFDM waveform, and Q radar receive antennas simultaneously receive the echos reflected off U targets during the communication downlink frame [8]. This architecture is mainly designed for vehicular systems, and hence, includes a continuous-wave radar with simultaneously operating transmit and receive antennas.

A. Communication Channel Model

Each UE is assumed to be randomly located in the cell; accordingly, the UEs may have significantly different channel gains. The path-loss of the kth UE is modeled as [9]

$$PL_k = 10\log_{10}\left(\frac{4\pi f_c d_0}{c_0}\right)^2 + 10\log_{10}\left(\frac{d_k}{d_0}\right)^{\varphi} + \zeta_{sh}, \quad (1)$$

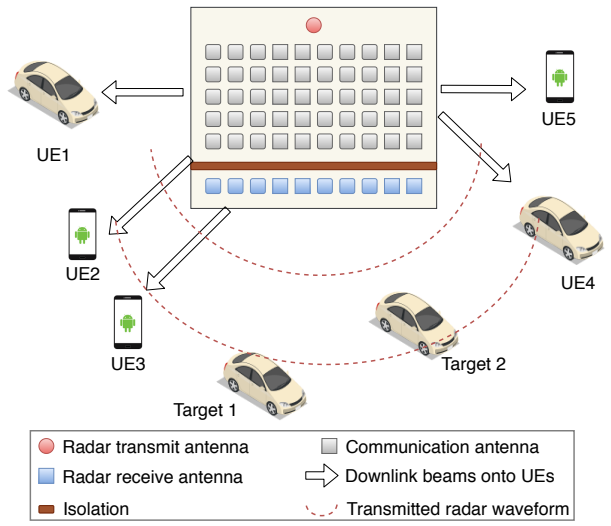

Fig. 1. A prototype system model where the base station (BS) communicates with downlink UEs via precoding while detecting the in-range targets simultaneously.

where f_c, d_0, c_0 and φ denote the frequency of the carrier signal, the reference distance, the speed of light and the path-loss exponent, respectively. Also, d_k is the distance of the kth UE to the BS, (i.e. $30 \leq d_k \leq 400$ m), and ζ_{sh} is the log-normal shadow fading which is a zero-mean Gaussian random variable with standard deviation σ_{sh}. In line with the non-line-of-sight (NLOS) urban macro-cell measurements in [9], the following parameters are used in the channel model: $f_c = 5$ GHz, $d_0 = 1$ m, $\varphi = 2.9$, and $\sigma_{sh} = 5.7$ dB. The large-scale fading of the kth UE is given by $\beta_k = 10^{-PL_k/10}$. The small-scale fading between the kth UE and the mth BS antenna is modeled as $f_{m,k} \sim \mathcal{CN}(0,1)$, which follows Rayleigh fading. The channel vector of the kth UE is given by $\mathbf{h}_k = \sqrt{\beta_k}\mathbf{f}_k \in \mathbb{C}^{M\times 1}$, where $\mathbf{f}_k = [f_{1,k}, \dots f_{m,k}, \dots, f_{M,k}]^T$. Also, let $\mathbf{H}_{com} \in \mathbb{C}^{M\times K}$ be the communication channel matrix between M BS antennas and K UEs, and $\mathbf{h}_{rad} \in \mathbb{C}^{1\times K}$ be the radar-communication interference channel vector between the radar transmit antenna and K UEs. The total communication and radar antenna output powers are denoted by p_{com} and p_{rad}, respectively.

B. Radar Channel Model

Radar channels are modeled as two-way LOS channels, as the signals transmitted by the radar are reflected off the target, and then received by the receive antennas. Assuming U targets in the radar range, the channel between the radar transmit antenna, uth target, and qth receive antenna is [5]

$$g_{u,q} = a_{u,q} e^{-j2\pi l \Delta f \Theta_u} e^{j2\pi f_{D,u} \mu t_o}, \tag{2}$$

where $\Theta_u = (R_{u,tx} + R_{u,q})/c_0$ denotes the phase shift due to the total path length $(R_{u,tx} + R_{u,q})$ from the radar transmit antenna to the target $R_{u,tx}$, and the target to the qth antenna element $R_{u,q}$. Moreover, l and Δf denote the subcarrier index and OFDM subcarrier spacing, respectively [5]. The second phase shift term given by $e^{j2\pi f_{D,u}\mu t_o}$ includes velocity information of the targets, where t_o is the duration of an OFDM symbol. The Doppler shift caused by the target velocity is given by $f_{D,u} = 2v_u f_c/\lambda$, where v_u denotes relative speed of the uth target, and λ denotes the wavelength of the signal. According to [10], the gain of the two-way channel between the radar transmit antenna, uth target, and qth radar receive antenna is given by

$$a_{u,q} = \frac{\lambda\sqrt{G_{tx}G_{rx}\sigma_u}}{(4\pi)^{3/2} R_{u,tx}R_{u,q}}, \tag{3}$$

where G_{tx} and G_{rx} are the gains of the transmit and receive antennas, respectively, and σ_u is the radar cross-section (RCS) of the target. The radar channel between the radar transmit antenna, and Q radar receive antennas is given by

$$\mathbf{g}_{rad} = \left[\sum_{u=1}^{U} g_{u,1}, \dots, \sum_{u=1}^{U} g_{u,q}, \dots, \sum_{u=1}^{U} g_{u,Q}\right] \in \mathbb{C}^{1\times Q}. \tag{4}$$

The communication downlink interference channel on the radar is given by $\mathbf{G}_{com} \in \mathbb{C}^{M\times Q}$, and each entry of $\mathbf{G}_{com}$ is given by $g_{m,q} = \sum_{u=1}^{U} g_{m,q,u}$, where each channel between the mth communication transmit antenna, U targets, and qth radar receive antenna calculated via (2).

III. Massive MIMO OFDM RadCom Architecture

A. RadCom Precoder

The transmitted symbol vector $\mathbf{y} \in \mathbb{C}^{M\times 1}$ by M communication antennas on the lth subcarrier during one symbol duration is written as

$$\mathbf{y} = \sqrt{p_{com}}\alpha_{ZF}\mathbf{W}_{\text{ZF}}^H \mathbf{\Delta}_K \mathbf{x}, \tag{5}$$

where, a zero-forcing (ZF) precoder is employed, as given by $\mathbf{W}_{ZF} = \left(\mathbf{H}_{com}^H \mathbf{H}_{com}\right)^{-1}\mathbf{H}_{com}^H$. Vector $\mathbf{x} = [x_1, \dots, x_k, \dots, x_K]^T \in \mathbb{C}^{K\times 1}$ denotes complex QAM symbols with average unit power, i.e. $\mathbb{E}\left[|x_k|^2\right] = 1$, which are transmitted by the BS to the K UEs. The power coefficient α_{ZF} is used to satisfy the power constraint of the precoded symbols, such that $\mathbb{E}\left[\|\mathbf{y}\|^2\right] = p_{com}$. Moreover, since the UEs are assumed to be randomly located in the network a power allocation matrix, given by $\mathbf{\Delta}_K = \text{diag}\left(\sqrt{\delta_1}, \dots, \sqrt{\delta_k}, \dots, \sqrt{\delta_K}\right) \in \mathbb{R}^{K\times K}$, is employed in (5) to control the power beam transmitted towards each UE. This power allocation matrix must satisfy the following total power condition,

$$\sum_{k=1}^{K} \mathbb{E}\left[\left\|\mathbf{w}_k^H\right\|^2\right] = \sum_{k=1}^{K} \mathbb{E}\left[\left\|\mathbf{w}_k^H\sqrt{\delta_k}\right\|^2\right], \tag{6}$$

where $\mathbf{w}_k \in \mathbb{C}^{1\times M}$ denotes the precoder vector of the kth UE, and its average power is $\mathbb{E}\left[\|\mathbf{w}_k\|^2\right] = \frac{1}{(M-K)\beta_k}$ for the ZF precoder [11]. Thus, the following condition is obtained,

$$\sum_{k=1}^{K} \frac{1}{\beta_k} = \sum_{k=1}^{K} \frac{\delta_k}{\beta_k}. \tag{7}$$

Since the radar transmits an OFDM waveform during downlink communication, the received signal vector by K UEs on the lth subcarrier under radar interference is given by

$$\widetilde{\mathbf{x}} = \underbrace{\mathbf{H}_{com}^{H}\mathbf{y}}_{useful\ signal} + \underbrace{\mathbf{h}_{rad}^{H}\sqrt{p_{rad}}s_{\mu,l}}_{radar\ interference} + \mathbf{n}, \tag{8}$$

where the transmitted radar symbol during this symbol duration on the lth subcarrier is denoted by $s_{\mu,l}$. Moreover, $\mathbf{n} = [n_1, \ldots, n_k, \ldots, n_K] \in \mathbb{C}^{K\times 1}$ denotes the complex Gaussian noise vector with zero mean and noise variance σ_n^2, i.e. $n_k \sim \mathcal{CN}\left(0, \sigma_n^2\right)$ at the kth UE. It can be seen in (8) that the radar interference at the UEs degrades the communication capacity. In turn, the following precoder is used to improve the capacity of the communication system by creating constructive interference at the UEs [8], as

$$\mathbf{y} = \sqrt{p_{com}}\widehat{\alpha}_{ZF}\mathbf{W}_{ZF}^{H}\Delta_k\mathbf{x} - \sqrt{\Psi p_{com}}\mathbf{W}_{ZF}^{H}\mathbf{h}_{rad}^{H}s_{\mu,l}, \tag{9}$$

where the first term indicates the useful communication signal, and the second term indicates the signal transmitted to exploit the radar interference. Moreover, Ψ denotes the power ratio between the radar and communication output powers, i.e. $p_{rad} = \Psi p_{com}$. This signal must still satisfy the output power constraint of the communication antennas, as given by

$$\mathbb{E}\left[\left\|\widehat{\alpha}_{ZF}\mathbf{W}_{ZF}^{H}\Delta_k\mathbf{x} - \sqrt{\Psi}\mathbf{W}_{ZF}^{H}\mathbf{h}_{rad}^{H}s_{\mu,l}\right\|^2\right] = 1. \tag{10}$$

Assuming that (7) is satisfied, Δ_k can be excluded from (10). In turn, $\widehat{\alpha}_{ZF}$ must be chosen as

$$\widehat{\alpha}_{ZF} = \sqrt{\frac{1 - \Psi\mathbb{E}\left[\left\|\mathbf{W}_{ZF}^{H}\mathbf{h}_{rad}^{H}\right\|^2\right]}{\mathbb{E}\left[\left\|\mathbf{W}_{ZF}\right\|_F^2\right]}}, \tag{11}$$

where $\mathbf{W}_{ZF}^{H}$ and $\mathbf{h}_{rad}^{H}$ are independent. Hence,

$$\mathbb{E}\left[\left\|\mathbf{W}_{ZF}^{H}\mathbf{h}_{rad}^{H}\right\|^2\right] \approx \mathbb{E}\left[\left\|\mathbf{W}_{ZF}^{H}\right\|_F^2\right]\mathbb{E}\left[\left\|\mathbf{h}_{rad}\right\|^2\right]\frac{1}{K}, \tag{12}$$

where $\mathbb{E}\left[\left\|\mathbf{h}_{rad}\right\|^2\right]\frac{1}{K} = \sum_{k=1}^{K}\frac{\beta_k}{K}$. Moreover, the Frobenius norm of the ZF is calculated as

$$\mathbb{E}\left[\left\|\mathbf{W}_{ZF}^{H}\right\|_F^2\right] = \sum_{k=1}^{K}\mathbb{E}\left[\left\|\mathbf{w}_k^{H}\right\|^2\right] = \sum_{k=1}^{K}\frac{1}{(M-K)\,\beta_k}, \tag{13}$$

and therefore,

$$\begin{aligned}\Psi\mathbb{E}\left[\left\|\mathbf{W}_{ZF}^{H}\mathbf{h}_{rad}^{H}\right\|^2\right] &\approx \Psi\sum_{k=1}^{K}\frac{1}{(M-K)\,\beta_k}\sum_{k=1}^{K}\frac{\beta_k}{K} \\ &\approx \frac{\Psi K}{M-K}.\end{aligned} \tag{14}$$

Accordingly, the analytical expression of $\widehat{\alpha}_{ZF}$ is given by

$$\widehat{\alpha}_{ZF} = \sqrt{(M-K-\Psi K)\left(\sum_{k=1}^{K}\frac{1}{\beta_k}\right)^{-1}}. \tag{15}$$

B. Optimum Radar Waveform Design

As proposed in [8], instead of transmitting a random radar waveform (RRWF), an optimum radar waveform (ORWF) can be selected by minimizing the distance between the communication symbols and the radar interference received at the UEs. The optimum radar waveform is obtained by solving the following optimization problem [8] ,

$$\underline{\mathcal{P}1:} \tag{16}$$

$$s_{\mu,l} = \underset{s_{\mu,l}}{\operatorname{argmin}}\ \left\|\widehat{\alpha}_{ZF}\mathbf{H}_{com}^{H}\mathbf{W}_{ZF}^{H}\Delta_k\mathbf{x} - \sqrt{\Psi}\mathbf{h}_{rad}^{H}s_{\mu,l}\right\|^2 \tag{16a}$$

$$\text{s.t.}\ \ \frac{\|\mathbf{S}\|_F}{NL} = 1, \tag{16b}$$

$$\left\|\widehat{\alpha}_{ZF}\mathbf{W}_{ZF}^{H}\Delta_k\mathbf{x} - \sqrt{\Psi}\mathbf{W}_{ZF}^{H}\mathbf{h}_{rad}^{H}s_{\mu,l}\right\|^2 = 1. \tag{16c}$$

While QAM modulation is used for the communication downlink, PSK modulation is employed in the OFDM radar waveform, and thus constraint (16b) is inherently satisfied via PSK-based radar waveform. The transmit power constraint (16c) of the communication antennas is satisfied by introducing a scaling factor, β_{ZF}, which is approximated by

$$\beta_{ZF} \approx \sqrt{\mathbb{E}\left[\left\|\widehat{\alpha}_{ZF}\mathbf{W}_{ZF}^{H}\Delta_k\mathbf{x} - \sqrt{\Psi}\mathbf{W}_{ZF}^{H}\mathbf{h}_{rad}^{H}s_{\mu,l}\right\|^2\right]^{-1}}. \tag{17}$$

Consequently, by substituting β_{ZF} and the optimum radar symbol into (9), the transmitted signal vector with optimum radar waveform is obtained as

$$\mathbf{y} = \sqrt{p_{com}}\beta_{ZF}\widehat{\alpha}_{ZF}\mathbf{W}_{ZF}^{H}\Delta_k\mathbf{x} - \mathbf{W}_{ZF}^{H}\sqrt{\Psi}\mathbf{h}_{rad}^{H}s_{\mu,l}. \tag{18}$$

IV. Analytical SINR Expression

It is assumed that the BS has perfect channel state information (CSI) and UE channels are uncorrelated for the sake of simplicity. Since the BS communicates with K UEs using the proposed precoder, and performs target detection with the optimum radar waveform target, the received signal at the K UEs is expressed as

$$\begin{aligned}\widetilde{\mathbf{x}} &= \mathbf{H}_{com}^{H}\sqrt{p_{com}}\beta_{ZF}\widehat{\alpha}_{ZF}\mathbf{W}_{ZF}^{H}\mathbf{\Delta_k}\mathbf{x} \\ &\quad - \mathbf{H}_{com}^{H}\sqrt{\Psi p_{com}}\mathbf{W}_{ZF}^{H}\mathbf{h}_{rad}^{H}s_{\mu,l} + \mathbf{h}_{rad}^{H}\sqrt{p_{rad}}s_{\mu,l} + \mathbf{n}.\end{aligned} \tag{19}$$

Based on (19), the received signal by the kth UE is given by (20), where $\mathbf{h}_{com,k}$ denotes the channel vector of the kth UE and $h_{rad,k}$ denotes the radar interference channel with the kth UE. The transmitted communication symbols have unit average power, and the radar waveform symbols (i.e. PSK symbols) have unit power, such that $\mathbb{E}\left[\left|x_k\right|^2\right] = 1$, and $\left|s_{\mu,l}\right|^2 = 1$. Thus, these symbol terms are not included in the power equations. Based on (20), the SINR of the signal at the kth UE can be calculated as given by (21). In the case

$$\hat{x}_k = \sqrt{p_{com}}\left(\sqrt{\delta_k}\beta_{ZF}\widehat{\alpha}_{ZF}\mathbf{h}_{com,k}^H\mathbf{w}_k^H x_k - \sqrt{\Psi}\mathbf{h}_{com,k}^H\mathbf{w}_k^H h_{rad,k}^* s_{\mu,l}\right) + \sqrt{p_{com}}\sum_{i=1,i\neq k}^{K}\left(\sqrt{\delta_i}\beta_{ZF}\widehat{\alpha}_{ZF}\mathbf{h}_{com,k}^H\mathbf{w}_i^H x_i - \sqrt{\Psi}\mathbf{h}_{com,k}^H\mathbf{w}_i^H h_{rad,i}^* s_{\mu,l}\right) + \sqrt{p_{com}\Psi}h_{rad,k}^* s_{\mu,l} + n_k. \quad (20)$$

$$SINR_k = \frac{\delta_k\beta_{ZF}^2\widehat{\alpha}_{ZF}^2\mathbb{E}\left[\left|\mathbf{h}_{com,k}^H\mathbf{w}_k^H\right|^2\right]}{\sum_{i=1,i\neq k}^{K}\mathbb{E}\left[\left|\mathbf{h}_{com,k}^H\mathbf{w}_i^H\left(\sqrt{\delta_i}\beta_{ZF}\widehat{\alpha}_{ZF} - \sqrt{\Psi}h_{rad,i}^*\right)\right|^2\right] + \Psi\mathbb{E}\left[\left|h_{rad,k}^*\right|^2\right]\mathbb{E}\left[\left|1 - \mathbf{h}_{com,k}^H\mathbf{w}_k^H\right|^2\right] + \sigma_n^2/p_{com}}. \quad (21)$$

of perfect CSI and $M \gg K$, $\mathbb{E}\left[\left|\mathbf{h}_{com,k}^H\mathbf{w}_k^H\right|^2\right] = 1$ and $\mathbb{E}\left[\left|\mathbf{h}_{com,k}^H\mathbf{w}_i^H\right|^2\right] = 0$, which results in the cancellation of inter-user interference and utilization of the radar interference at the UEs [8]. By substituting $\widehat{\alpha}_{ZF}$, given by (15) into (21), the SINR at the kth UE is obtained as

$$SINR_k = \frac{p_{com}\delta_k\beta_{ZF}^2\left(M - K - \Psi K\right)}{\sigma_n^2}\left(\sum_{k=1}^{K}\frac{1}{\beta_k}\right)^{-1}. \quad (22)$$

V. OFDM Radar and Target Detection

The received signal vector, $\mathbf{r}\left(\mu,l\right) = \left[r_1\left(\mu,l\right),\ldots,r_q\left(\mu,l\right),\ldots,r_Q\left(\mu,l\right)\right] \in \mathbb{C}^{Q\times 1}$, by Q radar receive antennas on the lth subcarrier with the μth transmitted symbol is given by

$$\mathbf{r}\left(\mu,l\right) = p_{com}\mathbf{g}_{rad}^H\Psi s_{\mu,l} + p_{com}\mathbf{G}_{com}^H\mathbf{y} + \mathbf{n}_Q,$$

where the first term refers the radar returns from the targets, the second term is the interference from the communication antennas, and $\mathbf{n}_Q \in \mathbb{C}^{Q\times 1}$ denotes the Gaussian noise with zero mean and variance σ_n^2 (i.e. $n_q \sim \mathcal{CN}\left(0,\sigma_n^2\right)$). The radar channel between the radar transmit antenna, the target, and the qth receive antenna is estimated by element-wise division of the received signal by the transmit radar symbol, as

$$\hat{g}_{rad,q}\left(\mu,l\right) = \frac{r_q\left(\mu,l\right)}{p_{com}\Psi s_{\mu,l}} = g_{rad,q}\left(\mu,l\right) + \frac{p_{com}\mathbf{g}_{com,q}^H\mathbf{y} + n_q}{p_{com}\Psi s_{\mu,l}}. \quad (23)$$

The transmitted radar waveform matrix consists of N 16-PSK symbols over L subcarriers (i.e. $\mathbf{S} \in \mathbb{C}^{N\times L}$), and thus, a processing gain of $G_p \triangleq NL$ is obtained after FFT/IFFT-based OFDM radar signal processing [5]. Thus, the average radar SINR after radar processing for the qth radar receive antenna is given by

$$\chi_{rad} = \frac{G_p p_{com}\Psi\mathbb{E}\left[\left|g_{rad,q}^* s_{\mu,l}\right|^2\right]}{U\left(p_{com}\mathbb{E}\left[\left|\mathbf{g}_{com,q}^H\mathbf{y}\right|^2\right] + \sigma_n^2\right)}, \quad (24)$$

where $\mathbb{E}\left[\left|s_{\mu,l}\right|^2\right] = 1$ for PSK symbols. The power of the communication interference on the radar return is given as

$$\mathbb{E}\left[\left|\mathbf{g}_{com,q}^H\mathbf{y}\right|^2\right] = p_{com}\mathbb{E}\left[\left|g_{com,q}^*\right|^2\right]. \quad (25)$$

Considering the radar channel model given in subsection II-B, it can be shown that $\mathbb{E}\left[\left|g_{rad,q}^*\right|^2\right] = \sum_{u=1}^{U}a_{u,q}^2$, and $\mathbb{E}\left[\left|g_{com,q}^*\right|^2\right] = \sum_{u=1}^{U}a_{u,q}^2$ for the U targets. Hence, the radar received SINR can be obtained as

$$\chi_{rad} = \frac{G_p p_{com}\Psi\sum_{u=1}^{U}a_{u,q}^2}{U\left(p_{com}\sum_{u=1}^{U}a_{u,q}^2 + \sigma_n^2\right)}. \quad (26)$$

Fig. 2 illustrates the estimated velocity-distance radar images of a single target with OFDM radar under communication interference, using symbol-based OFDM radar processing, as in [7]. The employed radar waveform consists of $N = 64$ 16-PSK symbols over $L = 1024$ subcarriers, and hence, the radar processing gain is $G_p = 48.2$ dB. The distance and velocity of the target are set as 200 m and 17 m/s, respectively, and the RCS of the target is $\sigma_u = 0$ dBm^2. It can be seen that the target cannot be detected easily when $\chi_{rad} < 20$ dB, while higher SINR provides better detection performance. In turn, the minimum radar image SINR is determined as $\chi_{rad} \geq 25$ dB to achieve a reasonable target detection performance.

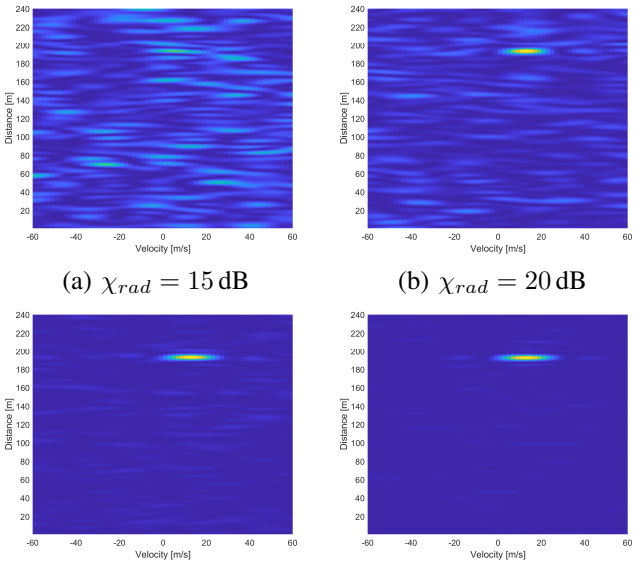

(a) $\chi_{rad} = 15$ dB (b) $\chi_{rad} = 20$ dB

(c) $\chi_{rad} = 25$ dB (d) $\chi_{rad} = 30$ dB

Fig. 2. Detection of a single target using OFDM radar with different SINRs.

VI. Optimum Beam Power Allocation

The ZF precoder tends to equalize the received powers at the UEs, however, this may limit the spectral efficiency of the system, as more power would be allocated to the beams towards the UEs with the worst channel conditions. Assuming p_{com} is fixed, the maximum SR can be achieved by solving

$$\underline{\mathcal{P}2:} \tag{27}$$

$$\max_{\Delta_K, \Psi} \quad C_{sum}\left(\Delta_K, \Psi\right) = \sum_{k=1}^{K} C_k\left(\delta_k, \Psi\right) \tag{27a}$$

$$\text{s.t.} \quad p_{rad} = \Psi p_{com}, \tag{27b}$$

$$\chi_{rad} \geq \chi_{min}, \tag{27c}$$

$$C_k\left(\delta_k, \Psi\right) \geq C_{min}, \quad \forall k = 1, \ldots, K, \tag{27d}$$

$$\sum_{k=1}^{K} \frac{1}{\beta_k} \geq \sum_{k=1}^{K} \frac{\delta_k}{\beta_k}, \tag{27e}$$

$$\delta_k \geq 0, \quad \forall k = 1, \ldots, K, \tag{27f}$$

$$\Psi \geq 0, \tag{27g}$$

where C_k is the achievable rate of the kth UE, expressed as

$$C_k\left(\delta_k, \Psi\right) = B \log_2\left(1 + SINR_k\left(\delta_k, \Psi\right)\right), \tag{28}$$

and $SINR_k$ is as defined in (22). Also, C_{min} is the minimum rate requirement per UE. In $\mathcal{P}2$, constraint (27b) determines the radar power output, while (27c) ensures that the minimum radar SINR is satisfied to detect the targets with the minimum target radar cross-section σ_{min} within the radar range R_{max}. Constraint (27d) ensures that each UE is served with at least C_{min} capacity, while (27f) ensures that the optimum power allocation does not change the total transmit power of the BS antennas. The last two constraints define the range of values of the decision variables. To reduce the complexity of problem $\mathcal{P}2$, χ_{rad} in (26) is used to determine the minimum value of Ψ, as

$$\Psi_{min} = 10^{\chi_{min}/10}\left(\frac{U\left(p_{com}\sum_{u=1}^{U} a_{u,q}^2 + \sigma_n^2\right)}{p_{com} G_p \sum_{u=1}^{U} a_{u,q}^2}\right), \tag{29}$$

where $a_{u,q}$ is given by (3). By setting $R_u = R_{max}$ and $\sigma_u = \sigma_{min}$, the minimum radar-communication power ratio Ψ_{min} can be computed, and thus $\Psi \geq \Psi_{min}$. In turn, constraint (27c) becomes redundant, and hence can be eliminated from problem $\mathcal{P}2$. In practical systems, the ratio of the radar output power to the communication output (i.e. $p_{rad} = \Psi p_{com}$) can be fixed, while ensuring that $\Psi \geq \Psi_{min}$, which implies that constraint (27b) can also be eliminated from problem $\mathcal{P}2$. For fixed Ψ (hence $p_{rad} = \Psi p_{com}$), it can be verified that the rate function of each UE is concave in δ_k, and the objective function $C_{sum}\left(\Delta_K\right)$ is also concave in Δ_K, since it is a linear sum of concave functions. Consequently, problem $\mathcal{P}2$ becomes a concave maximization problem, and hence, can be solved efficiently and optimally within polynomial-time complexity of $\mathcal{O}\left(K^2\right)$ via any standard convex optimization package [12].

TABLE I
Parameters of the RadCom system.

Parameter	Value	Description
B	100 MHz	Bandwidth
L	1024	Number of subcarriers
N	64	Number of symbols per radar waveform
T_{sym}	10.2 μs	Elementary symbol duration
T_{cp}	1.33 μs	Cyclic-prefix duration
T_O	11.53 μs	OFDM symbol duration
N_0	-174 dBm/Hz	Noise spectral density
σ_u	0 dBm^2	Target radar cross-section
G_{tx}, G_{rx}	3 dBi	Antenna gains

VII. Numerical Results

The simulation parameters are given in Table I. It is assumed that the desired maximum detectable target range is $R_{max} = 200$ m for a target with RCS $\sigma_u = 0$ dBm^2, as in vehicular radars. The communication cell radius is set as 400 m, since the BS may need to provide service to the UEs in a larger area. Note that the noise variance in dBm is calculated as $\sigma_n^2[\text{dBm}] = N_0 + NF + 10\log_{10} B$, where $NF = 7$ dB denotes the noise figure of the receivers. Hence, the noise variance in Watts is given by $\sigma_n^2 = 10^{\left(\sigma_n^2[\text{dBm}]-30\right)/10}$.

In the numerical results, the following schemes are defined. ZFR-ORWF and ZFR-RRWF indicate the proposed ZF-based radar interference utilization precoder (ZFR) with the optimum radar waveform (ORWF), and random radar waveform (RRWF), respectively. Moreover, ZFR-ORWF-OP and ZFR-RRWF-OP refer to the aforementioned schemes but with the optimum power (OP) allocation. Also, a minimum rate constraint C_{min} is defined for each UE. Consequently, ZFR-ORWF-OP ($C_k \geq C_{min}$) and ZFR-RRWF-OP ($C_k \geq C_{min}$) indicate that the minimum rate constraint is enforced per UE in the ZFR-ORWF-OP and ZFR-RRWF-OP schemes, respectively. Finally, ZF-WRI indicates the ZF precoder with radar interference, while ZF-WORI indicates the ZF precoder without considering the radar interference.

The analytical SR and radar SINR expressions derived in Sections IV and V are verified in Fig. 3, which shows a good agreement between the analytical and simulations results for all values of Ψ under all schemes. It can also be seen that increasing the radar-communication power ratio Ψ with the assistance of the radar processing gain G_p improves the radar SINR χ_{rad}, since the transmitted radar power also increases (i.e. $p_{rad} = \Psi p_{com}$). Moreover, a substantial SR gain is obtained when the optimum beam power allocation is employed, as seen in the comparison between ZRF-ORWF and ZRF-ORWF-OP, and also between ZRF-RRWF and ZRF-RRWF-OP. It is also observed that increasing Ψ to a certain value (i.e. $\Psi < 1$) improves the SR when ZRF-ORWF and ZRF-ORWF-OP are employed, as they can utilize the radar interference. On the other hand, excessively increasing Ψ degrades the SR due to the subsequent increase in radar interference, which may not be utilized entirely due to the limited power output of the communication antennas.

In Fig. 4, maximizing the SR is investigated under minimum

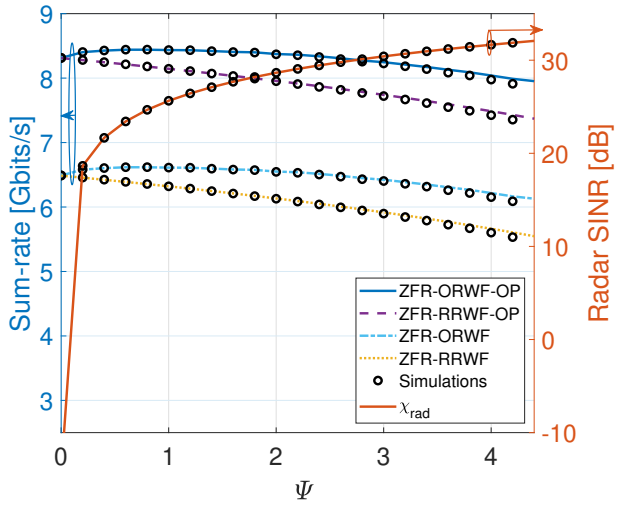

Fig. 3. Analytical and simulation results of SR and χ_{rad} w.r.t. radar-communication power ratio (Ψ) for $M = 100$, $K = 10$ and $P_{com} = 10$ W.

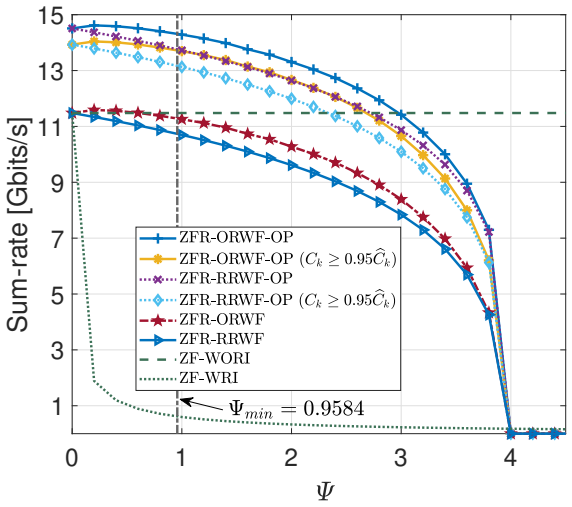

Fig. 4. SR of RadCom with different precoding and power allocation schemes w.r.t radar-communication power ratio. $M = 100$, $p_{com} = 10$ W, $K = 20$.

rate constraints per UE. The minimum rate constraint is given by $C_{min} = 0.95\widehat{C}_k$, where $\widehat{C}_k$ denotes the rate of the UEs that can be achieved without beam power allocation (i.e. via the ZRF-ORWF or ZRF-RRWF schemes). Evidently, the ZFR-ORWF-OP scheme outperforms all the other schemes, however, it does not guarantee that each UE can achieve the minimum rate requirement. Enforcing a minimum rate constraint slightly decreases the optimized SR, as seen in the comparison between ZFR-ORWF-OP and ZFR-ORWF-OP ($C_k \geq C_{min}$), and between ZFR-RRWF-OP and ZFR-RRWF-OP ($C_k \geq C_{min}$). The ZF-WORI is substantially outperformed by other schemes in terms of SR, since the ZF-WORI does not perform optimum power allocation over the beams, nor consider radar interference. Lastly, utilizing the ORWF provides a significant capacity gain over RRWF. For instance, a significant SR gain of about 3 Gbits/s is observed between ZFR-ORWF-OP and ZFR-ORWF, and between the ZFR-RRWF-OP and ZFR-RRWF schemes. This highlights the importance of optimal radar waveform design for the proposed precoder along with optimum downlink beam power allocation for maximizing the SR in massive MIMO RadCom systems.

VIII. Conclusion

In this paper, optimized massive MIMO OFDM RadCom precoders have been proposed for practical vehicular network scenarios, where the UEs and targets are randomly located in the network. Firstly, analytical expressions for the communication capacity and radar SINR have been derived. Using these expressions, the beam power allocation, radar-communication power ratio, and communication power output have been optimized to maximize the network SR, while guaranteeing the desired radar target detection SINR, and UEs' minimum rate requirements. The analytical results and robustness of the proposed scheme have been validated via numerical simulations, where it was shown that the proposed RadCom precoder substantially benefits from the optimum radar waveform design and optimum beam power allocation, in addition to exploiting radar interference to maximize the sum-rate.

References

[1] A. R. Chiriyath, B. Paul, and D. W. Bliss, "Radar-communications convergence: Coexistence, cooperation, and co-design," *IEEE Trans. on Cogn. Commun. Netw.*, vol. 3, no. 1, pp. 1–12, Mar. 2017.

[2] D. Ma, N. Shlezinger, T. Huang, Y. Liu, and Y. C. Eldar, "Joint radar-communication strategies for autonomous vehicles: Combining two key automotive technologies," *IEEE Signal Process. Mag.*, vol. 37, no. 4, pp. 85–97, July 2020.

[3] Q. Li, K. Dai, Y. Zhang, and H. Zhang, "Integrated waveform for a joint radar-communication system with high-speed transmission," *IEEE Wireless Commun. Lett.*, vol. 8, no. 4, pp. 1208–1211, Aug. 2019.

[4] F. Liu, C. Masouros, A. Li, H. Sun, and L. Hanzo, "MU-MIMO communications with MIMO radar: From co-existence to joint transmission," *IEEE Trans. Wireless Commun.*, vol. 17, no. 4, pp. 2755–2770, Apr. 2018.

[5] C. Sturm and W. Wiesbeck, "Waveform design and signal processing aspects for fusion of wireless communications and radar sensing," *Proceedings of the IEEE*, vol. 99, no. 7, pp. 1236–1259, July 2011.

[6] C. Sturm, Y. L. Sit, M. Braun, and T. Zwick, "Spectrally interleaved multi-carrier signals for radar network applications and multi-input multi-output radar," *IET Radar, Sonar Nav.*, vol. 7, no. 3, pp. 261–269, Mar. 2013.

[7] Y. L. Sit, B. Nuss, and T. Zwick, "On mutual interference cancellation in a MIMO OFDM multiuser radar-communication network," *IEEE Trans. Veh. Technol.*, vol. 67, no. 4, pp. 3339–3348, Apr. 2018.

[8] M. Temiz, E. Alsusa, and M. W. Baidas, "A dual-functional massive MIMO OFDM communication and radar transmitter architecture," *IEEE Trans. Veh. Technol.*, pp. 1–1, 2020.

[9] S. Sun and et al., "Investigation of prediction accuracy, sensitivity, and parameter stability of large-scale propagation path loss models for 5G wireless communications," *IEEE Trans. Veh. Technol.*, vol. 65, no. 5, pp. 2843–2860, May. 2016.

[10] M. A. Richards, J. A. Scheer, and W. A. Holm, Eds., *Principles of Modern Radar: Basic principles*. Institution of Engineering and Technology, 2010.

[11] H. Q. Ngo, E. G. Larsson, and T. L. Marzetta, "Energy and spectral efficiency of very large multiuser MIMO systems," *IEEE Trans. Commun.*, vol. 61, no. 4, pp. 1436–1449, Apr. 2013.

[12] S. Boyd and L. Vandenberghe, *Convex Optimization*. Cambridge University Press, 2003.